NGM 2016 Reykjavik
Proceedings of the 17th Nordic Geotechnical Meeting
Challenges in Nordic Geotechnic   25th – 28th of May

On the HVSR estimation at Icelandic strong-motion stations

B. Halldorsson
Earthquake Engineering Research Centre, University of Iceland, Selfoss, Iceland (skykkur@hi.is)
Faculty of Civil and Environmental Engineering, School of Engineering and Natural Sciences, University of Iceland, Reykjavík, Iceland. (EERC & FCEE, SENS, University of Iceland)

C. I. Olivera
ECS Mid-Atlantic, LLC, 6710 Oxon Hill Road, National Harbor, Maryland 20745, USA.

S. Rahpeyma, S. Ólafsson
EERC & FCEE, SENS, University of Iceland

R. A. Green
Department of Civil & Environmental Engineering, Virginia Tech, Blacksburg, VA, USA.

J.Th. Snæbjörnsson
School of science and engineering, Reykjavik University, Iceland

ABSTRACT
In this study Nakamura's H/V Spectral Ratio (HVSR) method was applied to ambient noise data and earthquake recordings collected at selected stations of the Icelandic Strong-motion Network (ISMN). In particular, continuous measurements of ambient noise, with minimum one-hour recordings, were performed while the strong-motion data set consisted of earthquake events recorded by the ISMN. The ambient noise data was analysed using various parameters such as time window duration, smoothing factor, different methods of averaging the two horizontal components and mean HVSR, respectively. For 20 minute recording window of ambient noise, applying the Konno and Ohmachi smoothing function with B = 20, combining the horizontal components and averaging the individual HVSR curves using the geometric mean, a stable HVSR amplification curve was obtained for a given site. The earthquake recordings were analysed using this common procedure by analysing the S phase instead of the entire time history. This unified procedure is applied in the HVSR method for characterization of the contribution of localized site effects at strong-motion stations in Iceland so that any similarities or differences observed can be attributed to factors other than data processing itself. The study serves as the first look at HVSRs at selected ISMN recording sites in Iceland using earthquake data. The results are expected to provide better insight into the localized site effects in view of the lack of geotechnical information which hampers the understanding of the relationship between Iceland's characteristic sub-surface materials and their dynamic response.

Keywords: HVSR, site effects, ISMN, lava, rock, soil.

1 INTRODUCTION

Iceland is located on the Mid-Atlantic Ridge, the diverging plate boundary of the North American and Eurasian plates in the North Atlantic Ocean. Crossing the island from southwest to north, the onshore part of the plate boundary shifts eastward, resulting in two transform zones: the South Iceland Seismic Zone, SISZ, which is completely onshore and the Tjörnes Fracture Zone, TFZ which is largely offshore. Destructive earthquakes in these regions have been well documented in historical annals of the last 1000 years. In the SISZ strong earthquakes up to magnitude 7 have repeatedly taken place in the past, generally as single events or sequences of magnitude 6-7 earthquakes every 100-120 years or so (Einarsson et al. 1981; Stefánsson and Halldórsson 1988; Einarsson 1991; Bjarnason et al. 1993; Stefánsson et al. 1993; Ambraseys and

Sigbjörnsson 2000; Pagli et al. 2003; Bellou et al. 2005). Consequently, the SISZ and TFZ are the regions in Iceland that have the greatest potential for the occurrence of large earthquakes, and thus, have the highest earthquake hazard (Sólnes et al. 2004). In fact, the most expensive natural disaster in Iceland was the 29 May 2008 $M_w6.3$ Ölfus earthquake in South Iceland which caused widespread damage. Site effects, or the amplification (or deamplification) of earthquake ground motion amplitudes, have long been known to be a major factor influencing the distribution of earthquake damage. In the official standard for earthquake resistant design in Iceland (Eurocode 8) the site effects are specified in terms of the average shear wave velocity in the uppermost 30 meters ($V_{S,30}$). The majority of the free-field stations of the Icelandic Strong-motion Network (ISMN) have thus been estimated to fall into the rock class ($V_{S,30} > 750$ m/s). However, this site classification has been based on surface geology because quantitative information on physical parameters of the geologic profile beneath the recording sites of the ISMN is virtually nonexistant.

Earthquake ground motions at a given site are often amplified over a narrow frequency range due to the dynamic response of local soil layers below the site. For particularly intense strong-motions, deamplification of high-frequency waves due to nonlinear soil behaviour may be observed. The large impedance contrast between the few tens of meters of soil and underlying bedrock has been shown to affect the amplification of seismic waves, somewhat disproportionally compared to the overall length of the propagation path from the source to site (Anderson et al. 1996; Boore and Joyner 1997). Where enough borehole and strong-motion data exists, e.g., in California, surface geology, which at least to the first approximation can be assumed to be representative of the of the uppermost few tens of meters of the geologic profile , has been found to correlate with $V_{S,30}$ (Wills et al. 2000). Surface geological mapping however cannot be expected to apply between regions with different geological evolutionary history and tectonic environment.

The surface geology of Iceland was formed during and after the last Ice Age. During the glacial period, Iceland was covered with a plateau glacier. It was not until the warmer interglacial periods and towards the end of the Pleistocene did sediment layers begin to form. As the glacier was retreating and the land rising, glacial streams formed thick sediment layers, composed primarily of sand and fine-grain gravel. In the postglacial period, some of those sediments were covered by lava, which added to the complexity of the geological structure of the surface in Iceland. Hence, in general, the surface geology of Iceland is described as a pile of basaltic lavas, as well as tuff layers, often with intermediate layers of sediments or alluvium (Einarsson and Douglas 1994). In addition, the surface geology is further complicated by fractures, fissures and faults of tectonic origin (Clifton and Einarsson 2005; Angelier et al. 2008). For practical purposes, the topsoil is easily removed resulting in most sites being considered as rock. However, a comprehensive study on site characterization at Icelandic strong-motion stations has not yet been carried out.

One of the most common procedures for estimating site effects, the horizontal-to-vertical spectral ratio (HVSR) method is based on recordings of ground shaking as a function of time in the horizontal, H, and vertical, V, directions, respectively, and calculating their amplitude as a function of frequency (Nakamura 1989). Analyzing the HVSR as a function of frequency allows one to capture the characteristics of the site conditions that may amplify earthquake shaking. Although the method's physical basis and theoretical background have been questioned (Lachetl and Bard 1994; Mucciarelli 1998), the advantages of the approach are several fold, foremost being that it is a relatively inexpensive and easy to implement for obtaining information needed in seismic hazard and risk analysis (Atakan et al. 1997; Bessason and Kaynia 2002).
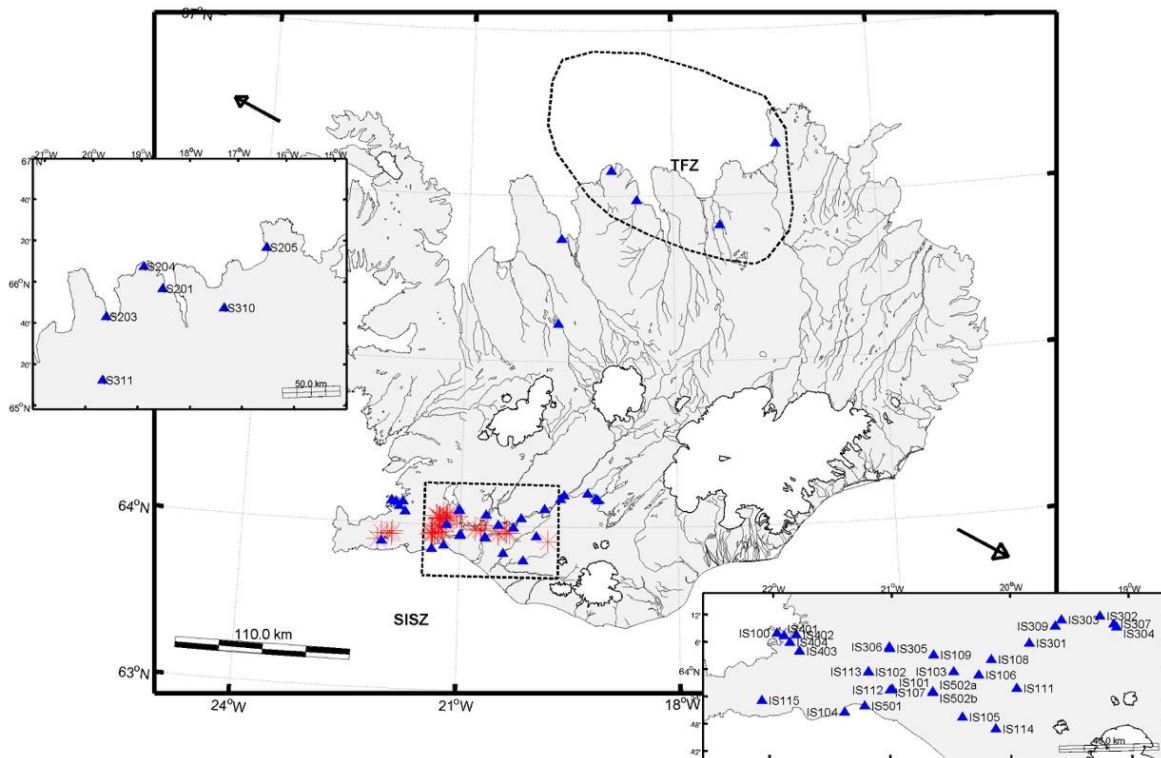
Figure 1. Stations of the Icelandic Strong-motion Network (represented by blue triangle symbols) and earthquake events (represented by red stars) recorded since its deployment (up to 2010). The inset picture at the bottom right shows the ISMN strong-motion stations along with station ID-codes with respect to the South Iceland Seismic Zone, SISZ, in the lowlands of south Iceland. The inset picture at the top left shows the ISMN strong-motion stations in the Tjörnes Fracture Zone, TFZ, in north Iceland.

The current study aims at investigating the characteristics of site response at selected strong-motion stations in Iceland shown in Figure 1. This study uses the HVSR method on earthquake data and can be considered as complementary to a study using microseismic data (Olivera et al. 2014). This study also augments the previous one by presenting results from a sensitivity analysis in determining the optimal parameters used in generating reliable HVSR from microseismic data, which were also used for estimating HVSR from earthquake data. As in the previous study, the aim is to estimate local site effects and relate to site characterization in terms of HVSR amplitudes and the corresponding predominant frequencies.

2 MICROSEISMIC DATA AND HVSR PARAMETER ESTIMATION

The guidelines published by SESAME for HVSR analysis (Bard and SESAME-Team 2005) were considered in this study in an

attempt to test the procedure for processing both ambient noise and earthquake data sets for HVSR analysis at Icelandic sites. For ambient noise data and earthquake recordings, the procedure would include all steps for HVSR analysis, from selecting a window length for analysis, merging the two horizontal components of the Fourier Amplitude Spectra, FAS, smoothing the combined horizontal, H, and vertical, V, components of the FAS, and calculating the mean HVSR for each site. The tests were carried out on the microseismic data recordings at four different stations exhibiting different HVSR signatures. Only the results for one station are shown herein, the Selfoss church station (IS117) which is located on lava rock but exhibits a clear HVSR predominant frequency corresponding to a relatively high amplification. For this purpose, continuous measurements of ambient noise with minimum one-hour recordings, were performed using a REF TEK 130-01 Broadband Seismic Recorder
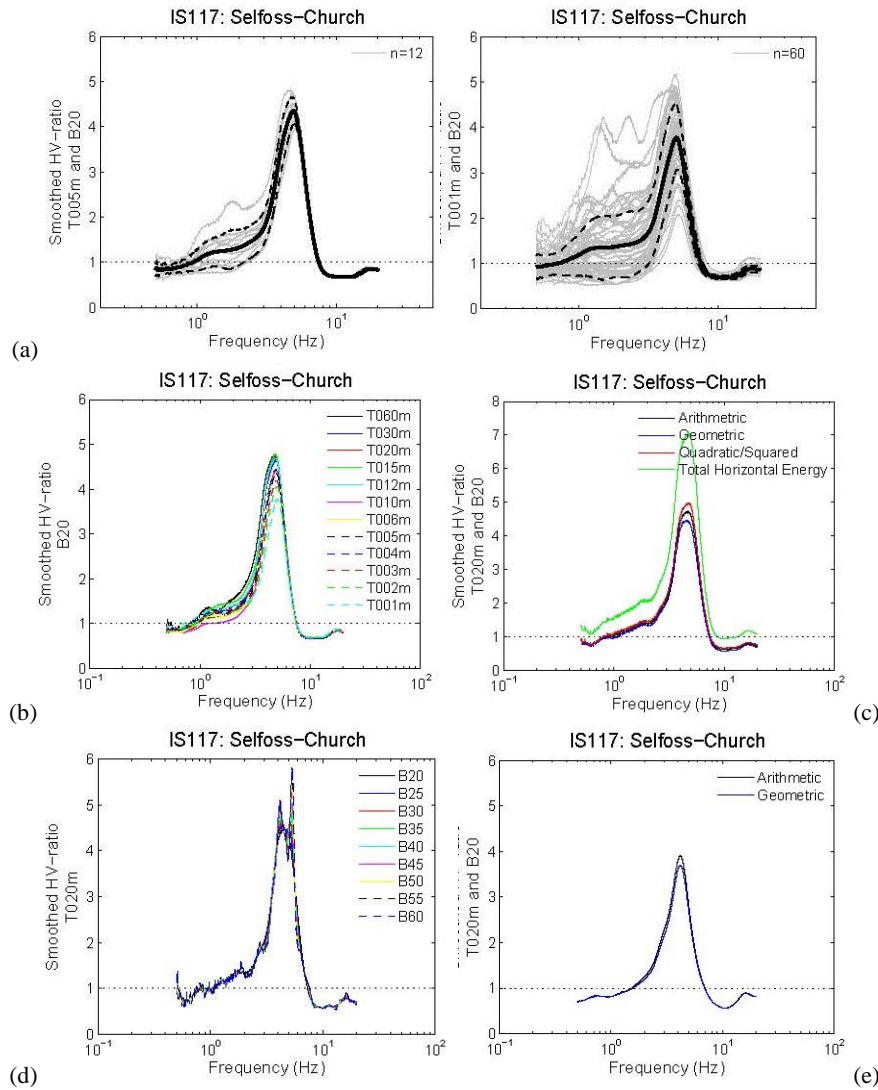
Figure 2. The HVSRs from test site IS117 used to investigate the effects of (a) different window lengths of 5 minutes (left) and 1 minute (right) for the same 60 minute microseismic recording, (b) (c), different methods for merging the horizontal components (d), different values for the Konno and Ohmachi smoothing coefficient, B (e), arithmetic and geometric mean on determining the mean HVSR, using twelve 20 minute time windows of ambient noise data.

and Lennartz LE-3D/5s Seismometer from the Icelandic instrument bank, Loki, which is operated through the Icelandic Meteorological Office, IMO.

One 60-minute recording of ambient noise was selected and divided into time windows of varying lengths (1, 2, 3, 4, 5, 6, 10, 12, 15, 20, 30, and 60 minutes) on which HVSR analyses were performed to determine the effects of various window lengths on the mean HVSR of a site. The variations of HVSRs of the different window lengths are shown for IS117 in Figure 2a. In an attempt to further investigate the influence of window lengths on the mean HVSR of a site, Figure 2b compares the mean HVSRs for all the window lengths considered. Despite the inconsistencies observed in Figure 2a, Figure 2b shows that the influence of the window length on the mean HVSR of this site is insignificant. These findings allowed the optimal window length of 20 minutes to be determined and used for HVSR analysis of ambient noise recordings. There is an increased inconsistency among individual HVSRs are found for window lengths shorter than 20 minutes.

For ambient noise data and earthquake recordings, the horizontal component of motion used in the HVSR method is obtained by combining the FAS of the two orthogonal horizontal components. The most commonly

used methods for combining both horizontal components in HVSR analysis are the following:

Arithmetic mean

$$H(f) = \frac{N(f) + E(f)}{2} \qquad (1)$$

Geometric mean

$$H(f) = \sqrt{N^2(f) * E^2(f)} \qquad (2)$$

Quadratic/Squared mean

$$H(f) = \sqrt{\frac{N^2(f) + E^2(f)}{2}} \qquad (3)$$

Total horizontal energy

$$H(f) = \sqrt{N^2(f) + E^2(f)} \qquad (4)$$

where $H(f)$ is the combined horizontal component FAS and $N(f)$ and $E(f)$ are the (two orthogonal) horizontal components of the FAS as a function of frequency, respectively.

In an effort to compare the above methods, a test was conducted at IS117 where one 20 minute time window of ambient noise was selected and HVSR analysis conducted using the four methods given by Equations (1) to (4). As observed in Figure 2c, HVSR results are consistent in overall general shape, predominant frequency, and amplification, except for the total horizontal energy method. Therefore, the geometric mean was selected to merge the horizontal components.

Prior to computing the HVSR the horizontal and vertical components can be smoothed (which in fact, is highly recommended and done in nearly all HVSR studies). The Konno and Ohmachi smoothing function is the most used and recommended for HVSR analysis (Konno and Ohmachi 1998):

$$S(f) = \left[\frac{\sin\left(B \cdot \log\left(\frac{f}{f_c}\right) \right)}{B \cdot \log\left(\frac{f}{f_c}\right)} \right]^4 \qquad (5)$$

where f is the frequency, f_c is the central frequency, and B is the bandwidth (or

smoothing) coefficient. The smoothing coefficient may vary between 0 and 100, where a coefficient 0 gives a very strong smoothing and a coefficient of 100 provides a very soft smoothing. To further investigate the effects of smoothing coefficients on HVSR analysis, one 20-minute time window of ambient noise was selected and smoothed using coefficients ranging from 20 to 60. The HVSR results from the test are presented in Figure 2d. The general overall shape, predominant frequency, and amplification are consistent irrespective of the smoothing coefficient applied in HVSR analysis. A smoothing coefficient of 20 was selected to smooth the combined horizontal component of the FAS for both ambient noise and earthquake recordings in HVSR analysis.

The final step in HVSR analysis is determining the mean HVSR for each measurement site. For both ambient noise and earthquake recordings, the mean HVSR for a site is determined by calculating the average of all the HVSRs computed for each selected time window. Although the geometric mean is the most commonly used, the arithmetic mean has also been used in HVSR studies. They are defined as follows:

Arithmetic mean

$$A(f) = \frac{\sum_{i=1}^{n} a_i(f)}{n} \qquad (6)$$

Geometric mean

$$A(f) = \sqrt[n]{\prod_{i=1}^{n} a_i(f)} \qquad (7)$$

where $A(f)$ is the mean HVSR of a site as a function of frequency, $a_i(f)$ is the HVSR for one time window, and n is the total number of available time windows used to derive the mean HVSR for each site. For station IS117 the results are shown in Figure 2e; the mean HVSRs are identical irrespective of the method used to complete the task. Therefore, the final mean HVSR for ambient noise and earthquake recordings for each site was determined by calculating the geometric mean of the HVSRs from all the available time windows at a measurement site.
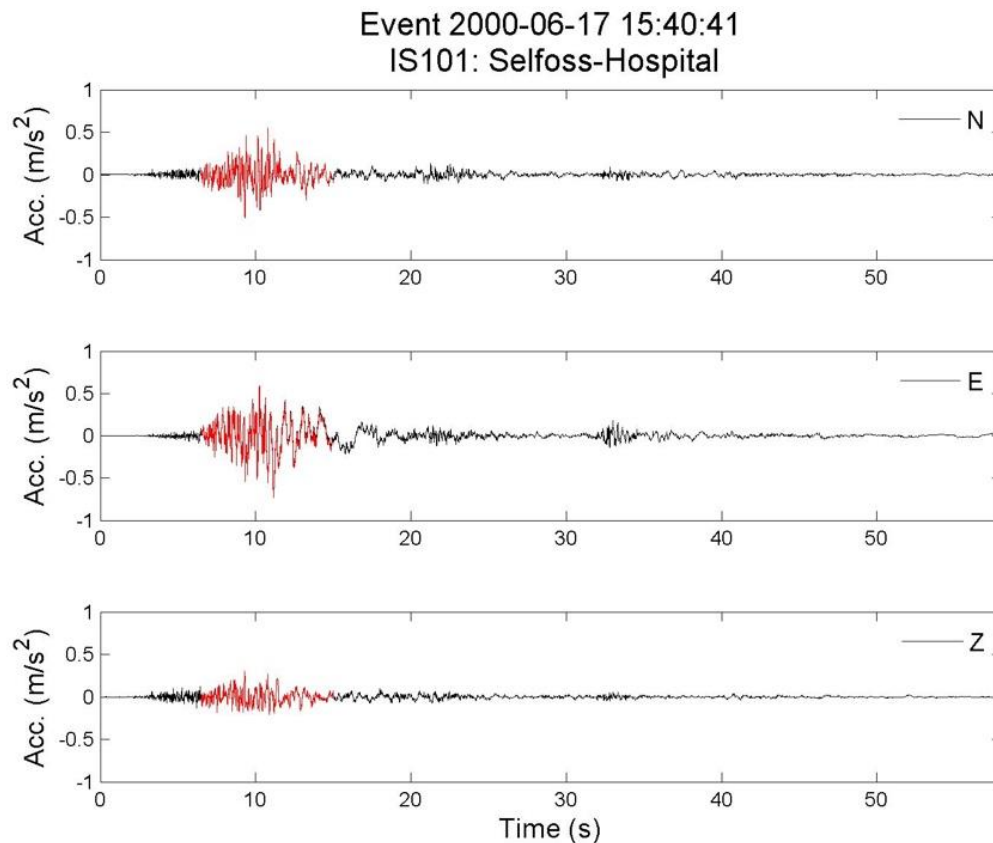
Figure 3. Recorded acceleration at ISMN station IS101 for the earthquake event of 17 June 2000 at 15:40 (M_w6.50, epicentral distance 30 km). The highlighted area indicates the S-phase of the recorded earthquake event on which HVSR analysis was conducted.

In this way a unified procedure was implemented to consistently process ambient noise data and earthquake recordings: (a) calculating the Fourier Amplitude Spectra for the selected time window and combining both horizontal components using a geometric mean, (b) applying the Konno and Ohmachi smoothing function with a smoothing coefficient of $B = 20$, and (c) creating a horizontal, H, to vertical, V, spectral ratio for the selected time window. The final mean HVSR for each site was determined by calculating the geometric mean of the HVSRs from all the individual time windows, from step (c) above. In this way, any similarities or differences observed can be attributed to factors other than data processing itself. For ambient noise data, 20 minute time windows were selected for HVSR analysis (Olivera et al. 2014), whereas for strong-motion data, the S phase of the earthquake recordings was selected as the time window for HVSR analysis.

3 STRONG-MOTION DATA

Over the past three decades the ISMN has collected hundreds of ground response time series (e.g., earthquake event recording shown in Figure 3) (see e.g., Table 2 in Sigbjörnsson et al. 2014). The recordings by the ISMN are accessible within the framework of the ISESD-project (Internet-Site for European Strong-Motion Data) (Ambraseys et al. 2004). Station locations (see Table 1 in Sigbjörnsson et al. 2014) were selected on the basis of the geographic distribution of the population and locations of industrial power plants, and main lifeline systems (Sigbjörnsson et al. 2004). The network consists of 40 permanent stations, approximately half of which are free-field (Sigbjörnsson et al. 2004; Sigbjörnsson and Ólafsson 2004). The instruments are located inside buildings for two reasons: (1) the severe climate conditions in Iceland make it difficult and expensive to operate sensitive
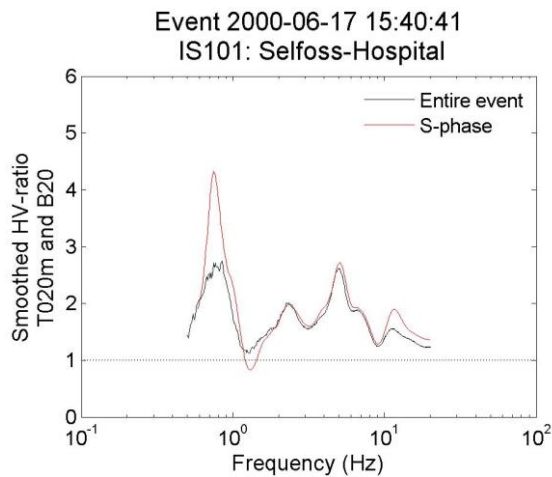
Figure 4. Comparison of the HVSRs computed over the entire earthquake event (black) and the S-phase only (red) of the acceleration time history shown in Figure 3.

equipment outdoors and (2) to ensure that the data obtained represent the direct seismic effects on the structural foundations. The instruments act in triggered mode detecting events when the ground acceleration exceeds a prescribed threshold (Sigbjörnsson et al. 2014).

In regards to earthquake recordings, the selection of the time window for HVSR analysis of strong-motion data required an investigation of the influence of different phases of an earthquake event on HVSR analysis, particularly the S phase. Previous studies using the HVSR method with strong-motion data have interchangeably used different parts of an earthquake recording. While some studies have used the entire earthquake recording (Mucciarelli et al. 2003; Triantafyllidis et al. 2006), most have concentrated on the S phase (Lermo and Chávez-García 1993) for HVSR analysis of strong-motion data because the S phase offers estimates of local amplifications in addition to predominant frequencies (Lermo and Chávez-García 1993). In the case of short source-to-site distances where it is difficult to separate the P and S arrivals, and thus difficult to isolate the S phase, studies have resorted to using the entire earthquake recording for HVSR analysis. In this study an investigation on the use of an entire recording versus the S phase for HVSR analysis was conducted. In general, minimal differences were observed when the time history used

contained the P, S, and coda waves versus only using the S waves and first part of coda. However, in some cases discrepancies were observed at low-frequencies, an example of which is shown in Figure 4 for the recording shown in Figure 3. Nevertheless, in this study the S phase of earthquake recordings is used in HVSR analysis.

4 RESULTS AND DISCUSSION

The results of the HVSR analysis on earthquake data at selected ISMN strong-motion stations are shown in Figure 5. The stations, numbered IS101 through IS112 are the oldest stations of the network and are all located in the SISZ, and station IS100 is located in Reykjavík. In general, the HVSRs appear to be quite variable. Nevertheless, and unlike the HVSR derived from microseismic recordings (Olivera et al. 2014), the reliability of the HVSRs derived from earthquake data appear to depend to some extent on the number of records used at each station. With the exception of stations IS100 and IS111 for which only one recording was used, IS107 for which only three were used, and for station IS112 where the individual HVSRs diverge at low frequencies, most stations appear to have relatively stable, near constant and low amplitude HVSR. Such characteristics were to be expected for rock sites. Notable exceptions however are seen at stations IS104, IS105, IS107, and IS109. Station IS104 is located on a relatively young (<10 th.y) and thin (a few tens of meters or less) lava rock which has been shown to produce a characteristic HVSR (Bessason and Kaynia 2002; Rahpeyma et al. 2016). Station IS105 is located on ancient seabed and river deposits of unknown thickness, and is classified as "stiff soil." Finally, station IS109 which also has been classified as "stiff soil" has a relatively flat near constant HVSR, characteristic of a "rock" site, apart from it exhibiting a curious peak above 10 Hz. However, the peak and the associated predominant frequency cannot be considered reliable due to the few observations used.

At some stations, especially Selfoss, Hveragerði, Thorlakshofn, Hella, and Tjorsartun there are multiple low-frequency
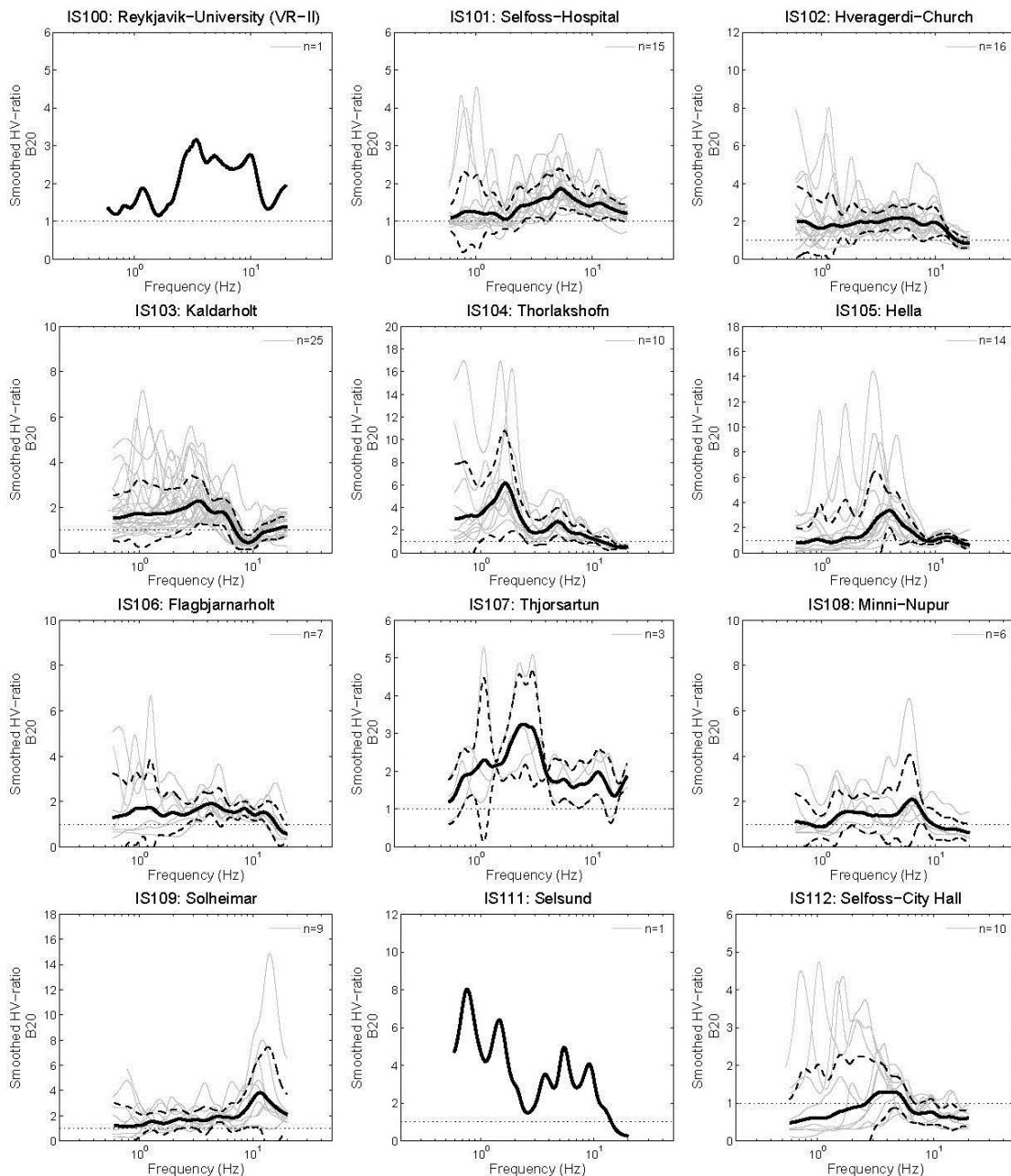
Figure 5. Mean HVSR +/- one standard deviation from earthquake recordings with a Konno and Ohmachi smoothing coefficient, B=20 where n is the number of available earthquake events used to derive the mean HVSR for the ISMN strong-motion stations.

HVSR peaks. The lack of a corresponding consistent predominant frequency at each site indicates that it is not a site characteristic. Rather, the low-frequency peaks are most likely due to intense low-frequency and large amplitude near-fault horizontal ground motions due to directivity effects and/or permanent tectonic displacements associated with the three strong earthquakes in 2000 and 2008. These results indicate that additional constraints are needed to validate the results, in particular accounting for obvious wave

effects from earthquake recordings (near-fault pulses, surface waves, etc.) and comparing with results from microseismic studies (Olivera et al. 2014).

5 CONCLUSIONS

Site effects are known to significantly affect outcrop earthquake strong-motions. The HVSR method has been shown to be a useful method for identifying dominant frequencies with respect to localized site

amplification and for classifying measurement sites. In the absence of HVSR analysis and geophysical data about the geologic profiles in Iceland at ISMN recording sites, most sites are classified as "rock" on the basis of surface geology.

This study is a part of a comprehensive effort of estimating HVSR at Icelandic strong-motion stations from microseismic data (Olivera et al. 2014) and from both earthquake and microseismic array data at recording sites of the Icelandic strong-motion arrays (Halldorsson et al. 2009; Halldorsson et al. 2012; Rahpeyma et al. 2016). It aims at establishing a clearer understanding of the site response by estimating reliable HVSRs for Icelandic strong-motion recording sites. Towards this end, we focus on establishing a consistent procedure for collecting and analyzing microseismic data and calculating the HVSRs. Using this procedure, we analyze earthquake recordings at selected stations of the ISMN and calculate their corresponding HVSRs. As expected for rock sites, most stations exhibit relatively constant HVSR (over the frequency range considered) of low amplitude. However, there appear to be significant exceptions to this trend, even for sites classified as rock. The results warrant a further study and comparison of HVSR from microseismic and earthquake data for all ISMN strong motion stations.

An example of such comparison is shown in Figure 6 for station IS104 in Thorlakshofn where the earthquake HVSR appears to have two predominant frequencies, one of about 2 Hz and another at 5-6 Hz, while the microseismic data only reproduces the peak at the lower predominant frequency. Such results need to be interpreted on the basis of as much geological and geotechnical information as possible. From shallow boreholes in the area the top layer is a relatively young lava rock with a softer sedimentary layer below (introducing a shear wave velocity reversal), and possibly repeating such "soil structure" at greater depths. The predominant frequencies of oscillation of such soil structure (considering a unit-area vertical column) with velocity reversals acting as flexible structural elements, can be efficiently modelled using
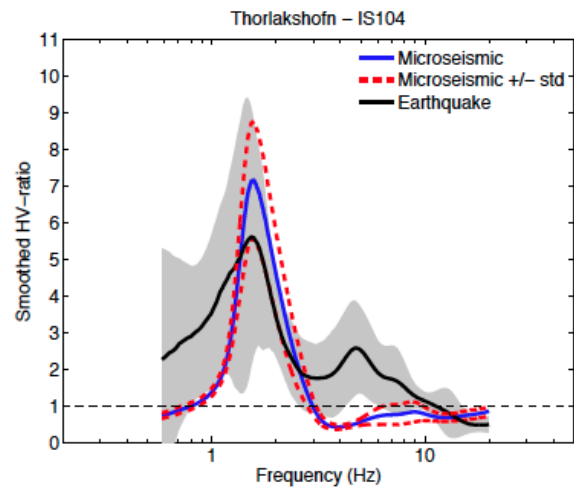

Figure 6. Mean HVSR and its 68-percentile limits from earthquake data (black solid line and shaded area) and microseismic data (blue solid line and red dashed lines) using smoothing coeff. B=20 at station IS104 in Thorlakshöfn, South Iceland.

dynamic response theory of a linear oscillator subjected to a base excitation (Rahpeyma et al. 2016).

6 ACKNOWLEDGEMENTS

7 REFERENCES

Ambraseys NN, Douglas J, Sigbjörnsson R, et al (2004) Dissemination of european strong-motion data, volume 2. In: Proceedings of the13th World Conference on Earthquake Engineering. p 13

Ambraseys NN, Sigbjörnsson R (2000) Re-appraisal of the seismicity of Iceland. Acta Polytechnica Scandinavica 2000-003:1–184.

Anderson JG, Lee Y, Zeng Y, Day S (1996) Control of strong motion by the upper 30 meters.

Bulletin of the Seismological Society of America 86:1749–1759.

Angelier J, Bergerat F, Stefansson R, Bellou M (2008) Seismotectonics of a newly formed transform zone near a hotspot: Earthquake mechanisms and regional stress in the South Iceland Seismic Zone. Tectonophysics 447:95–116.

Atakan K, Brandsdottir B, Halldórsson P, Fridleifsson GO (1997) Site response as a function of near-surface geology in the South Iceland Seismic Zone. Natural Hazards 15:139–164.

Bard PY, SESAME-Team (2005) Guidelines for the implementation of the H/V spectral ratio technique on ambient vibrations: measurements, processing, and interpretations. SESAME European research project.

Bellou M, Bergerat F, Angelier J, Homberg C (2005) Geometry and segmentation mechanisms of the surface traces associated with the 1912 Selsund Earthquake, Southern Iceland. Tectonophysics 404:133–149.

Bessason B, Kaynia AM (2002) Site amplification in lava rock on soft sediments. Soil dynamics and Earthquake engineering 22:525–540.

Bjarnason IT, Cowie P, Anders MH, et al (1993) The 1912 Iceland Earthquake Rupture: Growth and Development of a Nascent Transform System. Bulletin of the Seismological Society of America 83:416–435.

Boore DM, Joyner WB (1997) Site amplifications for generic rock sites. Bulletin of the Seismological Society of America 87:327–341.

Clifton A, Einarsson P (2005) Styles of surface rupture accompanying the June 17 and 21, 2000 earthquakes in the South Iceland Seismic Zone. Tectonophysics 396:141–159.

Einarsson P (1991) Earthquakes and present-day tectonism in Iceland. Tectonophysics 189:261–279.

Einarsson P, Björnsson S, Foulger G, et al (1981) Seismicity pattern in the South Iceland seismic zone. Earthquake Prediction 141–151.

Einarsson Þ, Douglas G (1994) Geology of Iceland: rocks and landscape.

Konno K, Ohmachi T (1998) Ground-motion characteristics estimated from spectral ratio between horizontal and vertical components of microtremor. Bulletin of the Seismological Society of America 88:228–241.

Lachetl C, Bard P-Y (1994) Numerical and Theoretical Investigations on the Possibilities and Limitations of Nakamura's Technique. Journal of Physics of the Earth 42:377–397.

Lermo J, Chávez-García FJ (1993) Site effect evaluation using spectral ratios with only one station. Bulletin of the Seismological Society of America 83:1574–1594.

Mucciarelli M (1998) Reliability and applicability of Nakamura's technique using microtremors: an experimental approach. Journal of earthquake engineering 2:625–638.

Mucciarelli M, Gallipoli MR, Arcieri M (2003) The Stability of the Horizontal-to-Vertical Spectral Ratio of Triggered Noise and Earthquake Recordings.

Bulletin of the Seismological Society of America 93:1407–1412.

Nakamura Y (1989) A method for dynamic characteristics estimation of subsurface using microtremor on the ground surface. Quarterly Report of Railway Technical Research Institute 30:25–33.

Olivera CI, Halldorsson B, Ólafsson S, et al (2014) A first look at site effects at Icelandic strong-motion stations using microseismic data. In: Proceedings of the 2nd European Conference on Earthquake and Engineering Seismology (2ECEES). Istanbul, Turkey,

Pagli C, Pedersen R, Sigmundsson F, Feigl KL (2003) Triggered fault slip on June 17, 2000 on the Reykjanes Peninsula, SWIceland captured by radar interferometry. Geophysical Research Letters 30:1273.

Rahpeyma S, Halldorsson B, Olivera CI, et al (2016) Site effect characterization of the Icelandic small-aperture strong-motion array (ICEARRAY I) in the presence of strong velocity reversals. Soil Dynamics and Earthquake Engineering (in review).

Sigbjörnsson R, Ólafsson S (2004) On the South Iceland earthquakes in June 2000: Strong-motion effects and damage. Bollettino di Geofisica teorica ed applicata 45:131–152.

Sigbjörnsson R, Ólafsson S, Rupakhety R, et al (2014) Strong-motion Monitoring and Accelerometric Recordings in Iceland. In: Proceedings of the 2nd European Conference on Earthquake and Engineering Seismology (2ECEES). Istanbul, Turkey,

Sigbjörnsson R, Ólafsson S, Thórarinsson Ó (2004) Strong-motion recordings in Iceland. In: Proceedings of the 13th World Conference on Earthquake Engineering. Mira, Vancouver, BC, Canada, p Paper no. 2370

Sólnes J, Sigbjörnsson R, Elíasson J (2004) Probabilistic seismic hazard mapping of Iceland: Proposed seismic zoning and de-aggregation mapping for EUROCODE 8. In: Proceedings of the 13th World Conference on Earthquake on Earthquake Engineering. p 14

Stefánsson R, Böðvarsson R, Slunga R, et al (1993) Earthquake prediction research in the South Iceland Seismic Zone and the SIL project. Bulletin of the Seismological Society of America 83:696–716.

Stefánsson R, Halldórsson P (1988) Strain release and strain build-up in the South Iceland seismic zone. Tectonophysics 152:267–276.

Triantafyllidis P, Theodulidis N, Savvaidis A, et al (2006) Site effects estimation using earthquake and ambient noise data: The case of Lefkas town (W. Greece). In: Procceedings of the 1st European Conference on Earthquake and Engineering Seismology (1ECEES), Geneva, Switzerland. pp 3–8

Wills CJ, Petersen M, Bryant WA, et al (2000) A site-conditions map for California based on geology and shear-wave velocity. Bulletin of the Seismological Society of America 90:S187–S208.